Research on Tunable Laser Temperature Measurement Method Based on Spectral Absorption

Ya-ping Li(✉) and Ming-fei Qu

College of Mechatronic Engineering, Beijing Polytechnic, Beijing 100176, China

Abstract. Traditional laser temperature measurement method has a slow warning speed because of its poor temperature measurement scheme. To solve this problem, a new tunable laser temperature measurement method is designed based on the spectral absorption process. According to the number of atoms, the gas molecular types are divided, and then the absorption line broadening is set based on the absorption process. On this basis, according to the relationship between the output light intensity and the incident light intensity, a tunable laser temperature measurement scheme is designed. In the experimental part, the measurement model of gas concentration and temperature field was constructed according to the absorption area ratio, and two temperature environments of −70 °C and 210 °C were set. According to the test results, the warning speed of this method is 3.39 min, 4.13 min and 7.43 min faster than the three groups of traditional methods at −70 °C, and 2.91 min, 4.08 min and 7.31 min faster than the three groups of traditional methods at 210 °C. Therefore, this method is more timely.

Keywords: Spectral absorption · Tunable laser · Temperature measurement model · Light intensity · Temperature field · Early warning effect

1 Introduction

In view of the importance of temperature field to combustion diagnosis, advanced and effective temperature measurement method has been a hot spot in the field of combustion research. For this reason, a high-precision wavelength tuning method of modulated grating Y-branch (mGy) tunable laser is designed in reference [1]. The temperature measurement is realized through high-precision wavelength scanning calibration of coarse scanning combined with fine scanning. According to the characteristics of tunable laser grating in reference [2], a new type of tunable distributed Bragg reflection laser based on sampling grating is designed. SG is used to replace the uniform grating of traditional DBR laser, and the temperature measurement and adjustment of different DBR laser tuning range are realized in a monolithic integrated chip.

On the basis of the above traditional methods, this paper introduces the application method of spectral absorption technology to further optimize the temperature measurement method. The method divides gas molecules according to the number of atoms,

S. Liu and X. Ma (Eds.): ADHIP 2021, LNICST 416, pp. 81–93, 2022.
https://doi.org/10.1007/978-3-030-94551-0_7

and then sets absorption line broadening based on spectral absorption process. Then according to the relationship between the light intensity and the incident light intensity, a tunable laser temperature measurement scheme is designed, so as to provide more reliable technical support for the temperature measurement in dangerous and complex environments.

2 Design of Tunable Laser Temperature Measurement Method

2.1 Classification of Gas Molecules

According to the number of atoms, molecules can be divided into diatomic molecules and polyatomic molecules. In addition to a small number of monatomic and diatomic molecules, most of gas molecules are polyatomic molecules. Therefore, the rotation of polyatomic molecules is studied. According to the interaction of rotation, vibration and electron motion, three mutually orthogonal directions passing through the molecular center of mass are selected, which are called the principal axes, and the corresponding moment of inertia is the principal moment of inertia. According to the different cases of moment of inertia, the molecular rotation can be divided into four categories: three principal moment of inertia are not equal, called asymmetric gyro molecules; two principal moment of inertia are equal, called symmetric gyro molecules; three principal moment of inertia are completely equal, called spherical gyro molecules; if the rotational inertia of the axis direction of the symmetric gyro is very small, the inertia ellipsoid is close to a circle Cylindrical molecules are called linear molecules. According to the degree of symmetry, linear molecules are divided into two types: centrosymmetric and noncentrosymmetric. Except for a few exceptions, the angular momentum of the electrons of linear polyatomic molecules in the ground state around the inter nuclear axis is zero, and the pure rotational energy level of the molecules is as follows:

$$\frac{E}{ab} = ZJ(J+1) - CJ^2(J+1)^2 \tag{1}$$

In formula (1): E represents rotational energy; a represents Planck constant; b represents speed of light; Z represents rotational constant; J represents rotational term; C represents constant term. $CJ^2(J+1)^2$ in formula (1) comes from the non rigidity of the molecule, which represents the influence of centrifugal force. Compared with $ZJ(J+1)$, it is very small, so it can be omitted [3]. The selection rule of rotational quantum number J for pure rotational spectra of linear molecules is $\Delta J = \pm 1$. Assuming that J' is a higher state and J'' is a lower state, then according to formula (1), the rotational spectrum of linear molecule can be expressed as:

$$g = F\left(J'\right) - F\left(J''\right) \tag{2}$$

Substituting $J' = J'' + 1 = J + 1$ into the above formula, we can get the following result:

$$g = 2Z(J+1) - 4C(J+1)^3 \tag{3}$$

According to the above formula, the pure rotational spectra of linear molecules are a series of spectral lines with approximately equal distance. For a symmetric gyro molecule, the two equal principal moment of inertia G_x and G_y are expressed by G_A, and the third principal moment of inertia G_z is expressed by G_B, then the molecular pure rotational energy level of the symmetric gyro molecule is:

$$F(J, W) = Z(J + 1) + (A - B)W^2 \tag{4}$$

In formula (4): A and B are the ratios of Planck's constants a and $8\pi^2$ and the speed of light to G_A and G_B; W represents the magnitude of the J component of the rotational quantum number. A symmetric gyroscope molecule has a symmetry axis, and the permanent dipole moment of the molecule is along the direction of the symmetry axis. The selection rule of W and J is:

$$\begin{cases} \Delta W = 0 \\ \Delta J = 0, \pm 1 \end{cases} \tag{5}$$

In pure rotational spectroscopy, the first set of conditions means that there is no transition, the transition at $\Delta J = J' - J'' = -1$ will not occur, and the transition will occur only at $\Delta J = +1$, that is, only those adjacent energy levels with the same W can merge with each other. The position of the spectral line of the infrared rotation spectrum of the symmetric gyro molecule is:

$$g = F\left(J', W'\right) - F\left(J'', W''\right) = 2Z(J + 1) \tag{6}$$

According to formula (6), the pure rotation spectrum of the symmetric gyro molecule is a set of equidistant spectral lines. If the molecule does not have a three-fold axis or a higher weight axis, all three principal moments of inertia are generally different. Such molecules are asymmetric gyroscopic molecules. Most polyatomic molecules are asymmetric gyroscopic molecules, which can be regarded as an intermediate situation between long symmetrical gyroscopic molecules and flat symmetrical gyroscopic molecules [4]. According to quantum mechanics, the energy level of asymmetric gyroscope molecules cannot be expressed as an explicit functional formula similar to the energy level formula of symmetric gyroscope molecules. The three main moments of inertia of the asymmetric gyro molecules are called G_A, G_B and G_C in the order of their increase, and are similar to the labeling method in the case of symmetric gyro molecules, and the following quantities are introduced:

$$A = \frac{a}{8\pi^2 b G_A}, B = \frac{a}{8\pi^2 b G_B}, C = \frac{a}{8\pi^2 b G_C} \tag{7}$$

If the molecule has a permanent dipole moment, in the case of dipole radiation, the choice of the rotational quantum number J is: $J = 0, \pm 1$. For asymmetric gyro molecules, transitions can occur between groups of energy levels belonging to different J values, and transitions can also occur between groups of energy levels belonging to a given J value at $\Delta J = 0$. Asymmetric gyro molecules have a large number of rotational transitions, and the rotational spectral lines are very rich. At present, only some very simple molecules have been studied in detail. The moments of inertia of the molecules

of the ball spinning around all axes passing through the center of mass are completely equal. The molecules simply rotate around a fixed axis in space, and the fixed axis can have any orientation relative to the molecule. The energy level of the ball gyro molecule can be obtained on the basis of the symmetric gyro molecule energy level formula (4). Let $G_A = G_B$, namely $A = B$, obtain the molecular pure rotational energy level of the ball gyro molecule as:

$$F(J) = ZJ(J+1) \tag{8}$$

In formula (8): J represents all values starting from 0, and the molecular energy depends on the quantum number J. Only when the molecule has a permanent dipole moment, the pure rotation spectrum can be produced. If the molecule has two or more symmetry axes, the permanent dipole moment of the molecule is zero, and the spherical gyro molecule does not display the infrared rotation spectrum. Divide the types of gas molecules according to the above formula.

2.2 Set Absorption Line Broadening Based on Spectral Absorption

Absorption line type can be used to describe the shape of absorption line in spectroscopy, which is a very important parameter when measuring gas concentration. The reason for the absorption line is that the energy of the gas molecule jumps to produce the absorption line. In an ideal state, the absorption line should be a straight line, but in actual situations, due to various interference factors, the absorption peak of the gas to be measured is a broad line type. The light absorption coefficient α of gas is related to the peak f of the linear function. Since the linear function is used to describe the change of the wavelength or frequency of the coefficient of the gas absorption spectrum, the peak f should be located at the center frequency of the function. Therefore, the light absorption coefficient α of gas can also be expressed as a normalized linear function centered on the center frequency of the spectral line, and its form is as follows:

$$\alpha(g) = Kf(g - g_0)N \tag{9}$$

The spread of spectral lines can be divided into three types of broadening: natural broadening, collision broadening and Doppler broadening. Among them, the natural broadening is determined by the nature of the molecule or atom itself, and it is caused by the instability of spontaneous radiation without being affected by the external environment [5]. The linear function of natural broadening is Lorentz type, and its linear function is:

$$f_L(g) = \frac{\Delta g_L}{2\pi} \frac{1}{(g - g_0)^2 + \left(\frac{\Delta g_L}{2}\right)^2} \tag{10}$$

In formula (10): g_0 represents the center frequency of different types; Δg_L represents the half-height width of the line type.

Collision broadening is caused by the collision between background molecules and radiation molecules. It is also caused by the instability of gas molecules in the excited state. Molecules will return to the ground state after a short residence time in the excited state. The residence time determines the characteristics of collision broadening. Therefore, the collision broadening is the same as the natural broadening, and their linear functions are Lorentz type. Doppler broadening is caused by the irregular motion of molecules or atoms in space, that is, the instability of molecules or atoms in space

$$f_G(g) = \frac{2}{g_G}\sqrt{\frac{\ln 2}{\pi}}\exp\left[-4\ln 2\left(\frac{g-g_0}{\Delta g_G}\right)^2\right] \tag{11}$$

In formula (11): Δg_G is the width at half height of Gaussian line [6]. So far, according to the characteristics of spectral absorption, the broadening of spectral line is set up.

2.3 Design of Tunable Laser Temperature Measurement Scheme

According to the Lambert Beer absorption law of spectrophotometry, the relationship between the intensity P of a beam of light passing through the absorption medium and the intensity P_0 of the incident light can be expressed as follows:

$$P = P_0\exp(-\beta D) = P_0\exp(-\eta N D) \tag{12}$$

In formula (12): β is the absorptivity; D is the absorption length; η is the absorption cross section; N is the particle number density of the absorption medium. The absorption cross section can be calculated by the following formula:

$$\eta = U(T)Qu(f) \tag{13}$$

In formula (13): $U(T)$ is the spectral line strength of the absorption medium, which is the inherent parameter of the absorption peak and is only related to the transition energy level and temperature; Q is the pressure; $u(f)$ is the linear function of $u(f)$ [7]. Substituting formula (13) into formula (12), the parameters after integration are obtained:

$$U(T)PNL = -\int \ln\left(\frac{P}{P_0}\right)dg \tag{14}$$

The right half of formula (14) is the integral absorptivity of the whole absorption peak. Because the absorption line strength of the medium is only a function related to temperature, the integral absorptivity of two different absorption peaks can be compared to eliminate the particle number density and pressure in the formula, and a new value of line strength a can be obtained. When the two selected absorption peaks are two different rotational transitions of the same vibrational band, the integral absorption ratio of formula (14) is finally obtained. The integral absorptivity of each absorption peak is $U(T)$ parameter that can be obtained by experimental measurement, and then the integral absorptivity θ can be obtained, so as to determine the relationship between the flame temperature and the measured value θ [8].

For the absorption spectrum temperature measurement technology, the selection of absorption spectrum line is very important, which should meet the following three basic principles: first, the interval between the two spectrum lines should not be too far or beyond the tuning range of the laser, and the spectrum line should be clean and free from the interference of other absorption spectrum lines; second, the selected absorption spectrum line should have a certain strength to ensure a good measurement signal-to-noise ratio; third, the selection of absorption spectrum line should have a good measurement signal-to-noise ratio The two absorption lines have proper lower level separation, which makes the measurement have enough temperature sensitivity.

2.4 Building the Measurement Model of Gas Concentration and Temperature Field

When the temperature distribution is known, the measurement model of gas concentration and temperature is constructed. In algebraic iterative reconstruction, the initial value of the iteration has a great influence on the reconstruction result. If the initial value of the iteration deviates too much, the reconstruction error will be large, and even the reconstruction result will be distorted. Therefore, the initial value close to the real value should be given as much as possible in the actual measurement reconstruction process. In order to give a reasonable two-dimensional distribution of gas concentration and temperature, tunable optical absorption signal is used to predict the gas concentration and temperature field. When two lasers with different wavelengths pass through the same test area, the path length and gas component concentration must be the same

$$\theta = \frac{S_1(T)}{S_2(T)} = \frac{S_1(T_0)}{S_2(T_0)} \exp\left[-\frac{ab}{m}(E_1 - E_2)\left(\frac{1}{T} - \frac{1}{T_0}\right)\right] \tag{15}$$

In formula (15): $S_1(T)$ and $S_2(T)$ denote the absorption area at the temperature of T; $S_1(T_0)$ and $S_2(T_0)$ denote the absorption area at the initial temperature of; m denotes the absorption strength; E_1 and E_2 denote the energy value under two conditions [9]. Then the actual value of absorption line wavelength is found in HITRAN database to determine the relationship between line strength and temperature. With the change of temperature, the line strength of the two absorption lines changes, and the relationship between the line strength ratio of the two absorption lines and the temperature is generated. According to the temperature relationship of line strength at different nodes, the range of line strength in the temperature field is determined, and the relationship between line strength and temperature in different intervals is analyzed [10]. As shown in Fig. 1, it is the schematic diagram of the measurement model for gas concentration and temperature field.

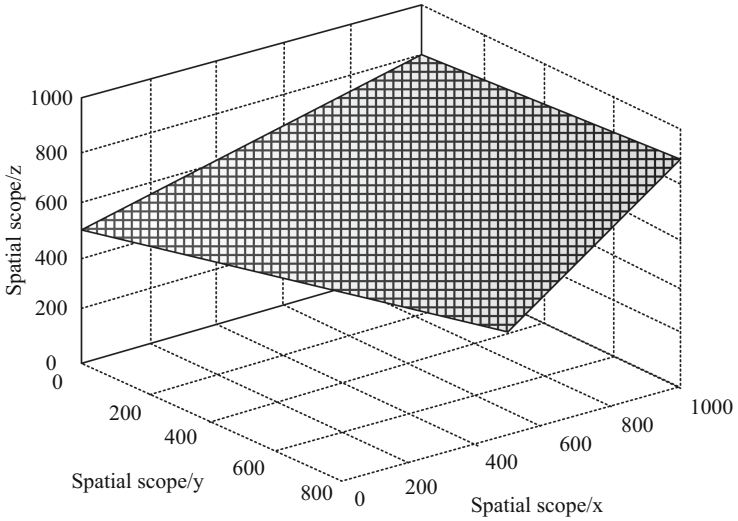

Fig. 1. Schematic diagram of gas concentration and temperature field measurement model

So far, the design of tunable laser temperature measurement method based on spectral absorption is completed.

3 Experimental Study

In order to verify the reliability of the tunable laser temperature measurement method based on spectral absorption, this method is compared with three groups of traditional temperature measurement methods, setting different temperature levels, comparing the temperature warning effect of the four groups of methods, and testing the temperature difference of the four methods.

3.1 Experimental Preparation

For this experimental test, an overall control circuit of the experimental operating system is constructed to perform the temperature measurement process of tunable laser. The accessories of the circuit mainly include: power adapter, RS-232 port, power indicator, single power level conversion chip, alarm, temperature sensor, matrix keyboard, memory, communication selection, function selection, trigger button, antenna, induction module, communication module, LCD, output indicator and power switch. On this basis, the serial port is debugged. Before debugging, connect the development board with the serial port line and power line, insert the SIM card on the back of the operating system circuit board, use the jumper cap to connect the communication, select the P and Q positions on the port, connect the power supply, press the trigger button and connect the wireless network. At this time, the system operation indicator starts to flash, which proves that the experimental system is established and can be applied to the temperature test. The parameters of the experimental platform are shown in Table 1.

Table 1. Experimental parameters

Serial number	Name	Parameter value
1	Temperature difference information	10 GB, 50 GB
2	System memory	32 GB
3	Working frequency	600 MHz
4	CPU main frequency	360 MHz

After setting the experimental parameters, the two groups of temperature field test environment were set as T1 and T2, and the temperature warning critical values of the two groups of environment were −70 °C and 210 °C respectively. The environmental temperature of the two groups was known, and reached the warning threshold value from the 5th min and the 9th min respectively. Four groups of temperature measurement methods were used to measure the temperature in the experimental environment.

3.2 Test Results at −70 °C

After debugging the experimental test system, real-time temperature measurement is carried out for the temperature change in the test background. The temperature measurement method designed in this paper is taken as experimental group A, and the three groups of traditional methods are taken as experimental group B, group C and group D respectively. Figure 2 shows the measurement results of four methods when the critical temperature is −70 °C.

As can be seen from Fig. 2, group a began to recognize abnormal temperature from the 5th, 32th min, and quickly reached the critical value of early warning. However, the three groups of traditional methods only warned the abnormal temperature from 8.45 min, 9.16 min and 12.5 min respectively. In order to ensure the authenticity, reliability and universality of the experimental test data, a total of 8 rounds of tests were carried out at this stage, and the results are shown in Table 2.

According to Table 2, the average values of the four groups of test data are 5.13 min, 8.52 min, 9.26 min and 12.56 min respectively. Comparing the four groups of test results, it is found that the warning speed of the temperature measurement method designed in this paper is 3.39 min, 4.13 min and 7.43 min faster than the three groups of traditional methods respectively.

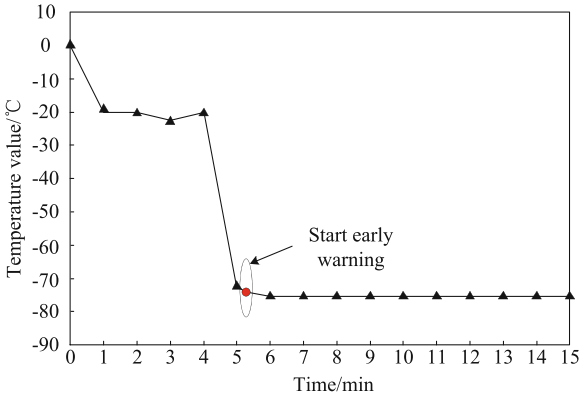

(a) Experimental group A

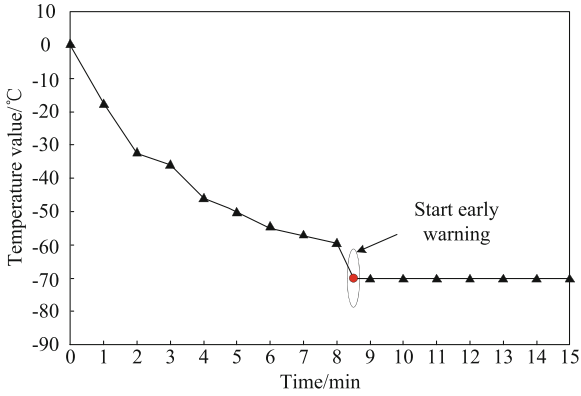

(b) Experimental group B

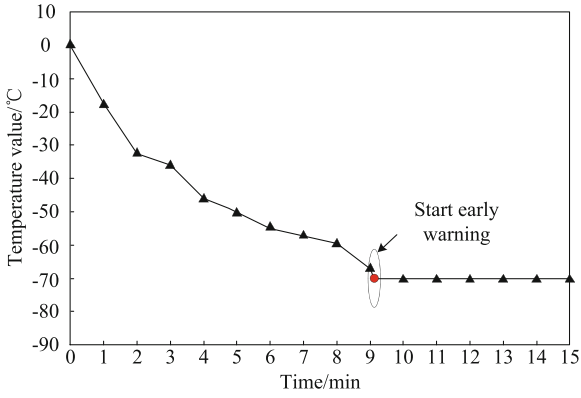

(c) Experimental group C

Fig. 2. Test results at −70 °C

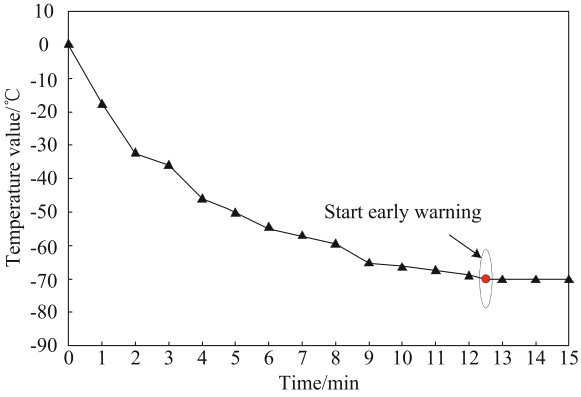

(d) Experimental group D

Fig. 2. continued

Table 2. Temperature warning speed test (min)

Test group	Group A	Group B	Group C	Group D
1	5.32	8.45	9.16	12.5
2	5.07	8.48	9.25	12.63
3	5.15	8.52	9.49	12.58
4	5.04	8.63	9.29	12.44
5	5.11	8.54	9.08	12.47
6	5.10	8.55	9.22	12.69
7	5.06	8.49	9.34	12.58
8	5.22	8.48	9.27	12.55

3.3 Test Results at 210 °C

Keep the basic test conditions unchanged and change the test environment to 210 °C. Figure 3 shows the measurement results of four methods when the critical temperature is 210 °C.

According to the curve change trend in Fig. 3, the designed temperature measurement method has the fastest warning speed in the face of high temperature test. Similarly, 8 rounds of tests were conducted, and the temperature warning results of each round are shown in Table 3.

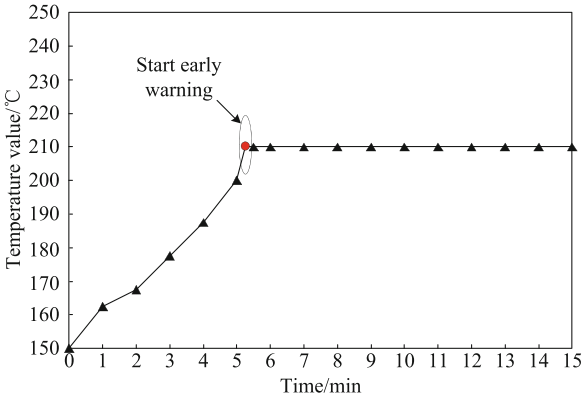

(a) Experimental group A

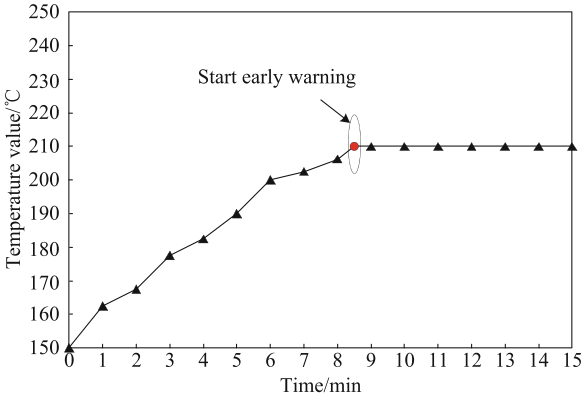

(b) Experimental group B

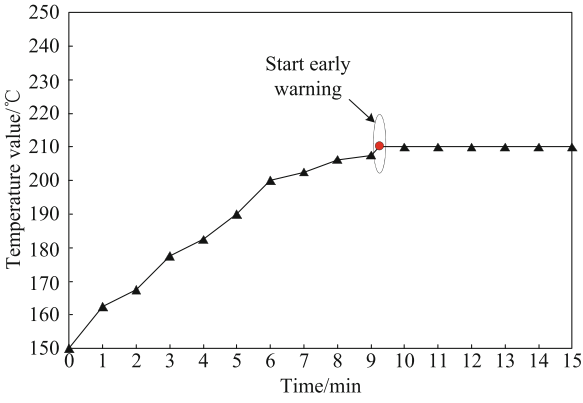

(c) Experimental group C

Fig. 3. Test results at 210 °C

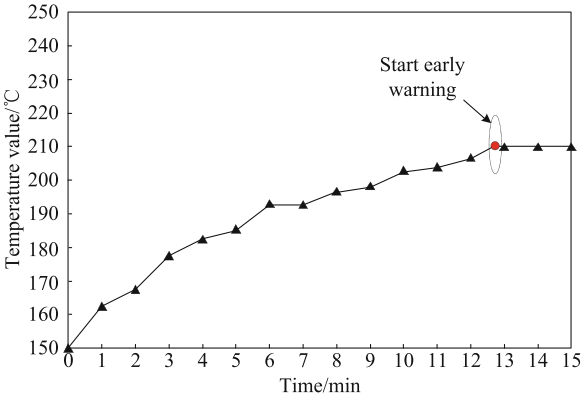

(d) Experimental group D

Fig. 3. continued

Table 3. Temperature warning speed test (min)

Test group	Group A	Group B	Group C	Group D
1	5.35	8.55	9.24	12.63
2	5.29	8.29	9.33	12.58
3	5.14	8.54	9.25	12.6
4	5.22	5.76	9.28	12.62
5	5.25	8.55	9.37	12.55
6	5.3	8.52	9.41	12.49
7	5.24	8.47	9.4	12.46
8	5.18	8.61	9.35	12.58

According to Table 3, the average warning time of the four groups was 5.25 min, 8.16 min, 9.33 min and 12.56 min, respectively. According to the above calculation results, when the critical temperature is 210 °C, the warning speed of the designed temperature measurement method is 2.91 min, 4.08 min and 7.31 min faster than the three methods respectively. Based on the above two sets of test results, it is verified that the temperature measurement method designed in this paper has good temperature warning effect in high temperature and low temperature environment.

4 Conclusion

On the basis of traditional temperature measurement methods, the tunable laser temperature measurement technology is optimized by means of spectral absorption, which provides a more reliable technical means for the current temperature measurement.

However, due to the limitation of research time, the method in this paper still has some deficiencies. For example, the amount of calculation is too large, and the calculation of various data is completed under the guidance of a large number of formulas, so there may be some calculation errors. Therefore, in the future research, it will be considered to design a supplementary detection module for real-time testing of various data to improve the reliability of temperature measurement results.

Fund Projects. Doctoral project of Beijing Polytechnic,A tunable laser temperature measurement method based on spectral absorption (2017Z004-006-KXZ).

References

1. Lv, X., Zhao, J., Xiong, Y., et al.: Design and study of a sampled gratings based tunable DBR laser. Study Opt. Commun. **12**(06), 47–51 (2019)
2. Zheng, S., Yang, Y.: High precision and accuracy wavelength tuning characteristics of modulated grating Y-branch tunable lasers. Chin. J. Lasers **46**(02), 9–16 (2019)
3. Zheng, W., Xie, R., Lu, Y., et al.: Study on crystal morphology and gas molecular transport mechanism of flammable ice generation process. Shanghai Energy Cons. **25**(02), 135–139 (2019)
4. Zhang, J., Ma, H., Ma, L., et al.: First-principles study on modulation mechanism of the electronic structures and magnetic properties of CdG by gas molecules adsorption. J. Synth. Cryst. **48**(06), 1030–1039 (2019)
5. Chen, S., Song, T., Yin, X.: Research on long-range hydrogen sulfide gas concentration detection system based on spectral absorption principle. Chin. J. Electron. Dev. **43**(04), 736–740 (2020)
6. Zhang, B., Xu, Z., Liu, J., et al.: absorption model of wavelength modulation spectroscopy in combustion flow field. Chin. J. Lasers **46**(07), 300–306 (2019)
7. Su, C., Yan, C., Wang, F., et al.: Research on error compensation method for infrared temperature measurement under laser irradiation. J. Appl. Opt. **40**(06), 1084–1090 (2019)
8. Liu, S., Liu, D., Srivastava, G., Połap, D., Woźniak, M.: Overview and methods of correlation filter algorithms in object tracking. Complex Intell. Syst. **7**(4), 1895–1917 (2020). https://doi.org/10.1007/s40747-020-00161-4
9. Liu, S., Lu, M., Li, H., et al.: Prediction of gene expression patterns with generalized linear regression model. Front. Genet. **10**, 120 (2019)
10. Liu, S., Bai, W., Zeng, N., et al.: A fast fractal based compression for MRI images. IEEE Access **7**, 62412–62420 (2019)